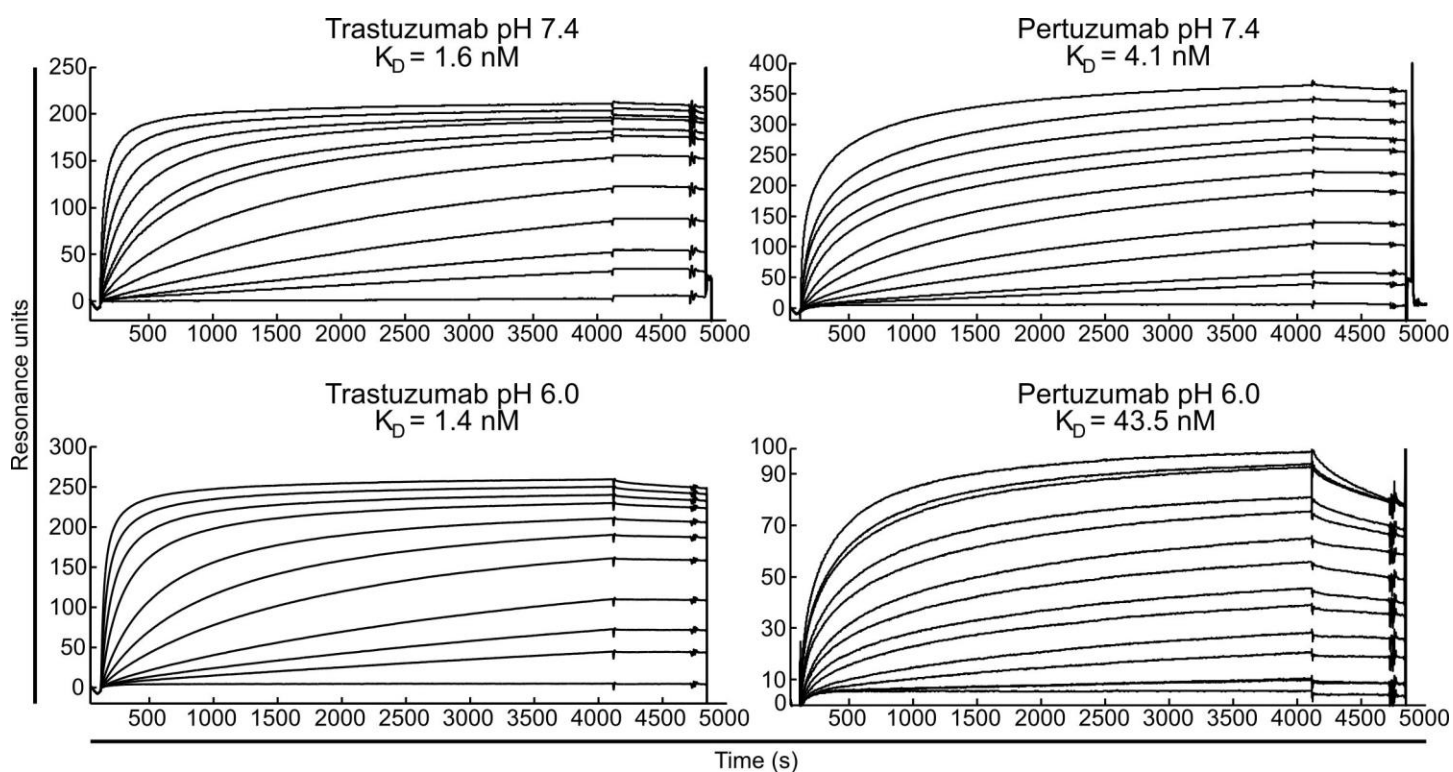


In the format provided by the authors and unedited.

# Engineering a HER2-specific antibody–drug conjugate to increase lysosomal delivery and therapeutic efficacy

Jeffrey C. Kang<sup>1,6</sup>, Wei Sun<sup>1,6</sup>, Priyanka Khare<sup>1,6</sup>, Mostafa Karimi<sup>2</sup>, Xiaoli Wang<sup>1</sup>, Yang Shen<sup>2</sup>, Raimund J. Ober<sup>1,3,4\*</sup> and E. Sally Ward<sup>1,4,5\*</sup>

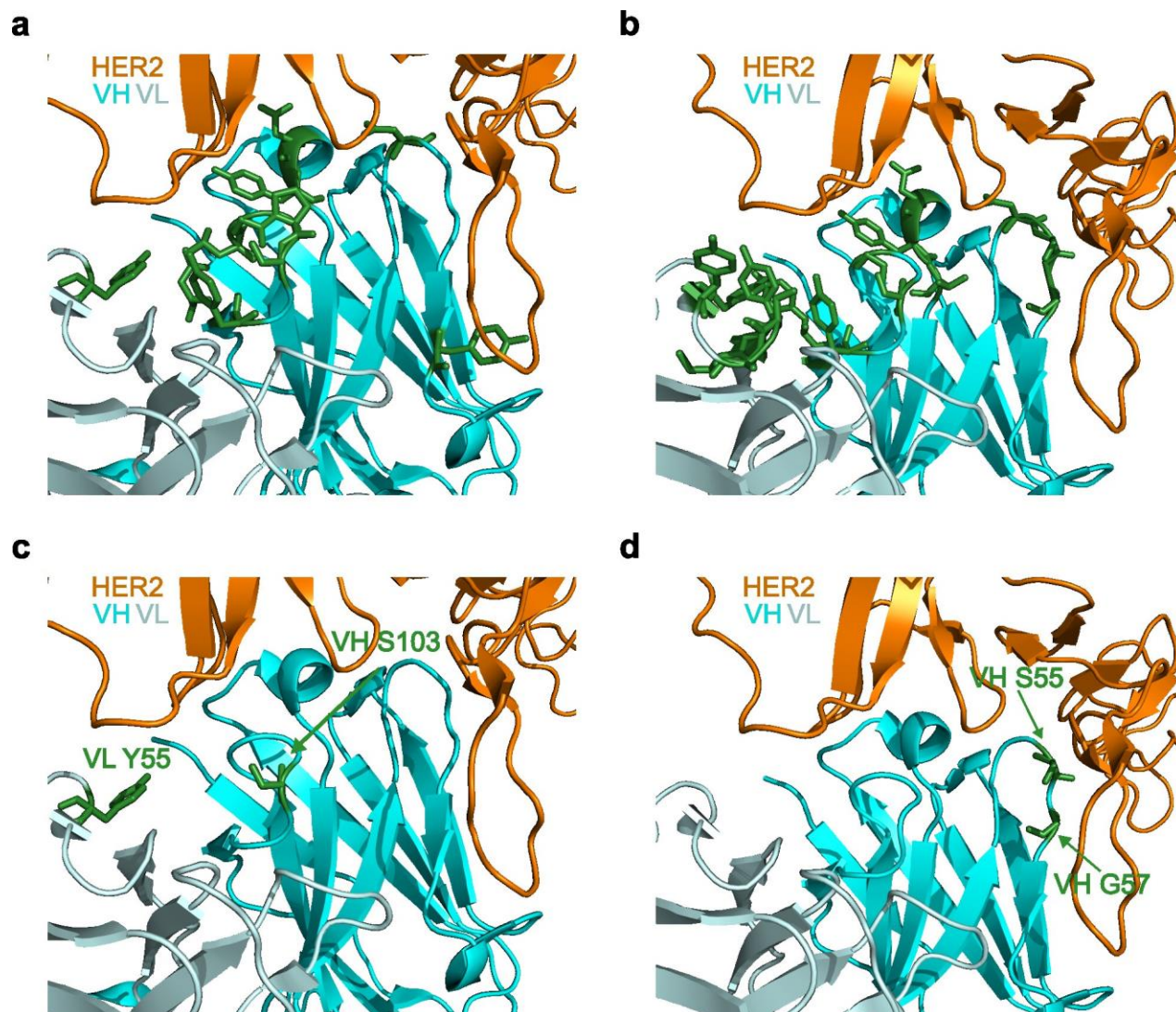
<sup>1</sup>Department of Molecular and Cellular Medicine, Texas A&M University Health Science Center, College Station, TX, USA. <sup>2</sup>Department of Electrical & Computer Engineering, Texas A&M University, College Station, TX, USA. <sup>3</sup>Department of Biomedical Engineering, Texas A&M University, College Station, TX, USA. <sup>4</sup>Cancer Sciences Unit, Centre for Cancer Immunology, Faculty of Medicine, University of Southampton, Southampton, UK. <sup>5</sup>Department of Microbial Pathogenesis and Immunology, Texas A&M University Health Science Center, Bryan, TX, USA. <sup>6</sup>These authors contributed equally: Jeffrey C. Kang, Wei Sun, Priyanka Khare \*e-mail: [raimund.ober@tamu.edu](mailto:raimund.ober@tamu.edu); [sally.ward@tamu.edu](mailto:sally.ward@tamu.edu)



**Supplementary Figure 1**

Surface plasmon resonance analyses of the interaction of clinical grade trastuzumab or clinical grade pertuzumab with immobilized recombinant human HER2 extracellular domain fused to Fc (HER2-ECD).

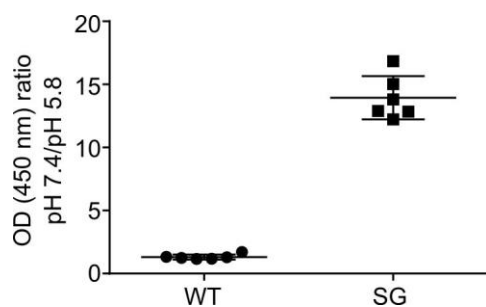
Antibodies were injected at either pH 7.4 or 6.0 at concentrations ranging from 0.25-2,200 nM and equilibrium dissociation constants ( $K_D$ s) determined. Representative traces for duplicate or triplicate injections for each analyte concentration are presented. At least two independent experiments with similar results were carried out for each interaction.



**Supplementary Figure 2**

Strategy for generating acid-switched variants of pertuzumab.

The X-ray crystallographic structure of the pertuzumab:HER2 extracellular domain complex (Protein Data Bank: 1S78) is shown, with the pertuzumab VH domain, VL domain and HER2 domain II shown in cyan, light cyan and orange, respectively. Residues targeted for mutagenesis by histidine replacement (a) or for production of phage display libraries (b) are shown in green. (c) Residues Tyr55 (CDRL2) and Ser103 (CDRH3) that were mutated to histidine to generate the YS mutant are shown in green. (d) Residues Ser55 (CDRH2) and Gly57 (CDRH2) that were mutated to His and Glu, respectively, to generate the SG mutant are displayed in green.



### Supplementary Figure 3

Binding behavior of phage bearing WT pertuzumab or SG mutant, as single-chain Fv fragments (scFvs).

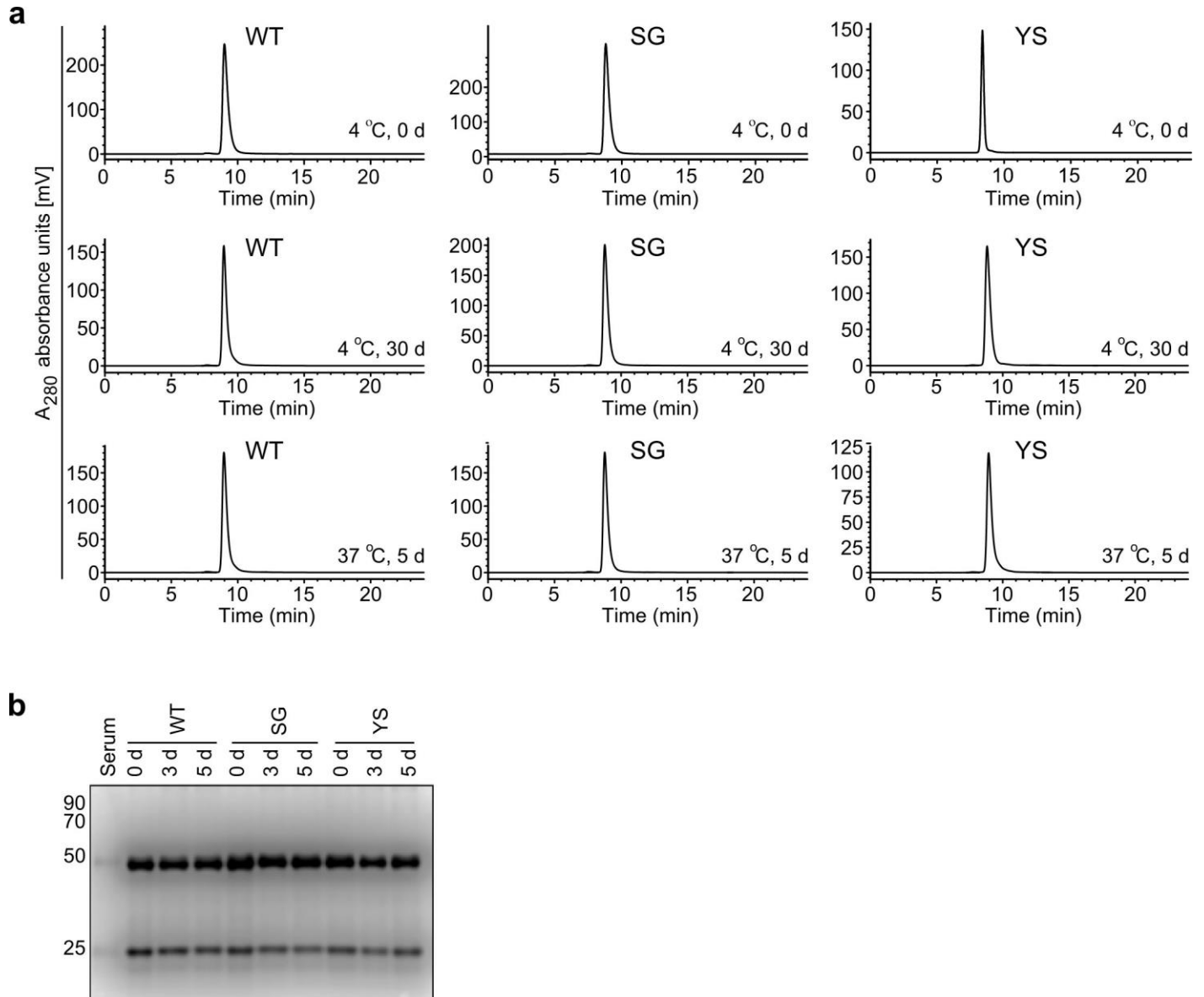
Phage-displayed scFvs (WT or SG mutant) were analyzed for binding to HER2-ECD at pH 7.4 and 5.8 using ELISA. The ratio of signal measured at pH 7.4 to pH 5.8 was calculated. The data shown is the mean ratio of a total of 6 independent samples  $\pm$  SD for each phage type/pH derived from two independent experiments.

| Antibody | K <sub>D</sub> (nM) |      |       |                          |
|----------|---------------------|------|-------|--------------------------|
|          | pH                  |      |       |                          |
|          | 7.4                 | 7.0  | 6.5   | 5.8                      |
| WT       | 2.9                 | 5.9  | 27.2  | 137.6                    |
| YS       | 6.3                 | 22.1 | 67.9  | ~1.6 x 10 <sup>3</sup> * |
| SG       | 4.7                 | 46.4 | 172.7 | N.D.**                   |

#### Supplementary Figure 4

Surface plasmon resonance analyses of the binding of WT pertuzumab and mutated variants YS and SG to HER2.

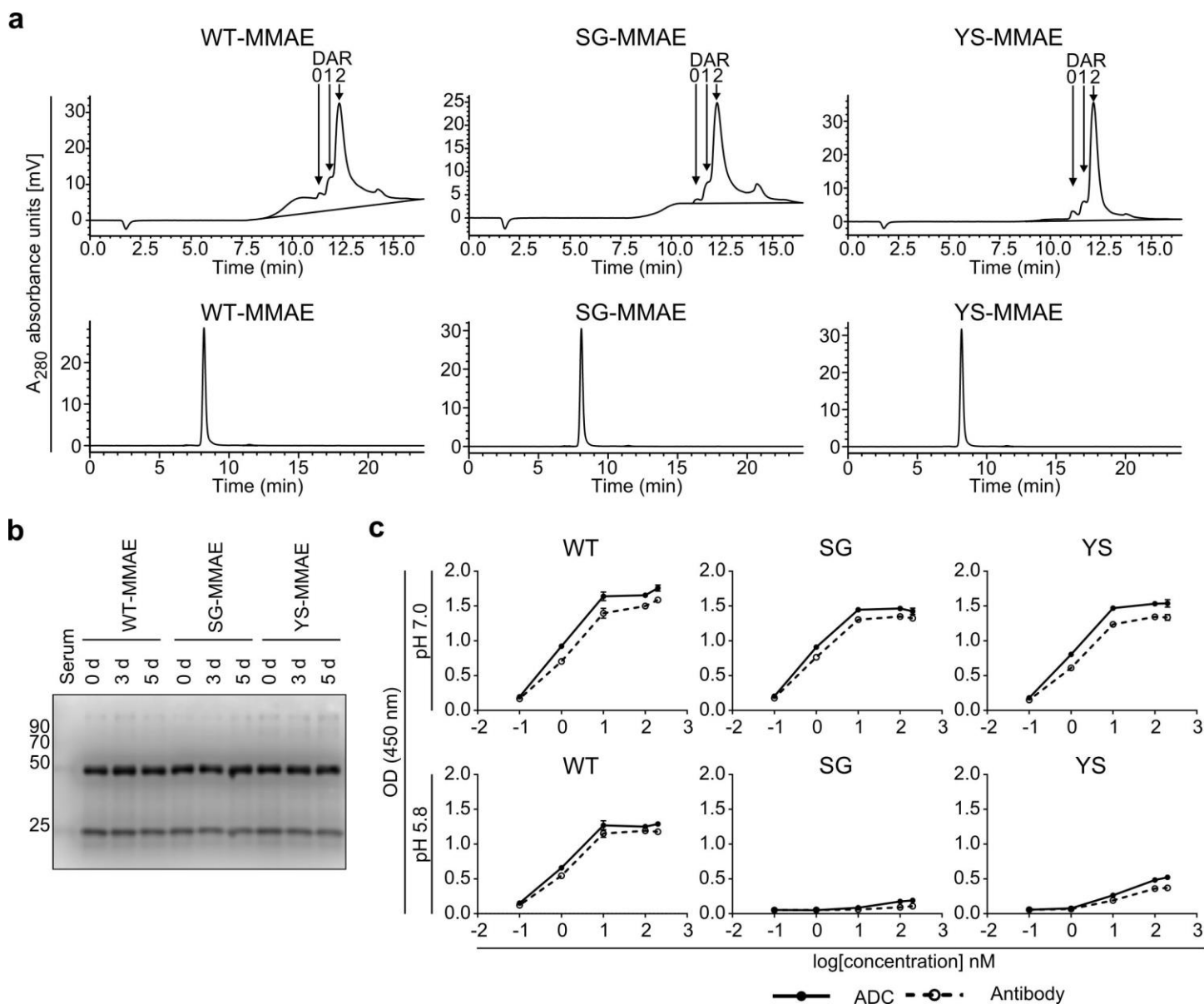
Equilibrium dissociation constants (K<sub>D</sub>s) for the interactions of the antibodies with immobilized recombinant human HER2 extracellular domain fused to Fc (HER2-ECD) were determined at pH 7.4, 7.0, 6.5 and 5.8. \* estimated binding affinity from the amount bound at equilibrium (see Methods). \*\* N.D., not determined, since binding too low to estimate a dissociation constant. Two independent experiments with similar results were carried out for each interaction.



### Supplementary Figure 5

Stability analyses of WT pertuzumab and SG, YS mutants (as full-length human IgG1/ $\kappa$  antibodies).

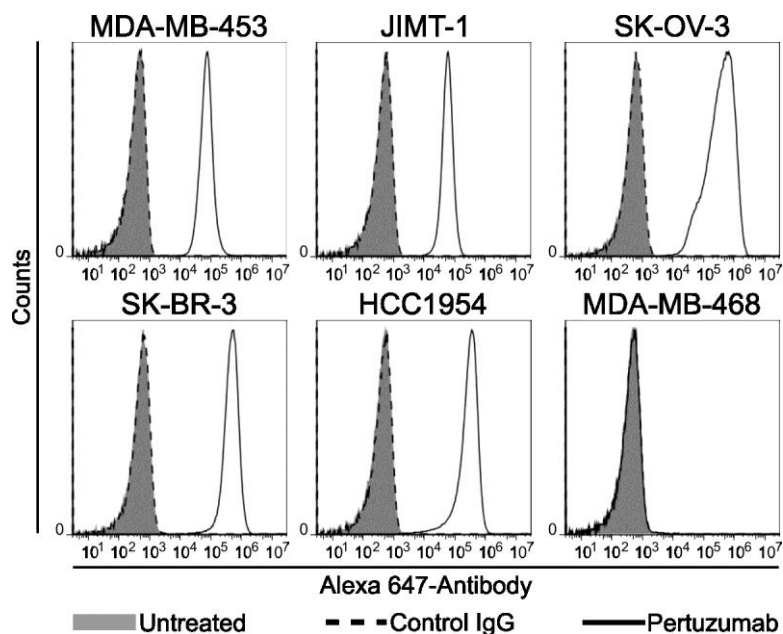
(a) WT pertuzumab or SG, YS mutants were stored at 4 °C for 0 days, 4 °C for 30 days, or 37 °C for 5 days and analyzed using size exclusion chromatography. (b) WT pertuzumab or SG, YS mutants were incubated in IgG-depleted, human serum for 0, 3, or 5 days at 37 °C. Antibodies were immunoprecipitated and analyzed by immunoblotting (serum indicates control sample without antibody added). Sizes of molecular weight markers (in kDa) are shown on the left margin. Two independent experiments were carried out with similar results.



### Supplementary Figure 6

Characterization of WT pertuzumab and acid-switched mutants (SG, YS) following conjugation to MMAE.

(a) MMAE-conjugated antibodies (WT-MMAE, SG-MMAE or YS-MMAE) were analyzed using a hydrophobic interaction column to determine the drug-to-antibody ratio (upper row). Analyses of MMAE-conjugated antibodies using size exclusion chromatography are also shown (lower row). (b) WT-MMAE, SG-MMAE or YS-MMAE were incubated in IgG-depleted human serum for 0, 3, or 5 days at 37 °C. Following incubation, ADCs were immunoprecipitated and analyzed by immunoblotting (serum indicates control sample without ADC added). Sizes of molecular weight markers (in kDa) are shown on the left margin. (c) Antibodies (WT, SG and YS) and their respective MMAE-conjugated ADCs were analyzed for binding to HER2-ECD using ELISA at pH 7.0 and 5.8. Mean values for independent triplicate sample wells are shown and error bars indicate SD. For panel (a), at least 3 (YS-MMAE) or 4 (SG-MMAE or WT-MMAE) preparations of ADC were analyzed with similar results. For panels (b) and (c), two independent experiments were carried out with similar results.

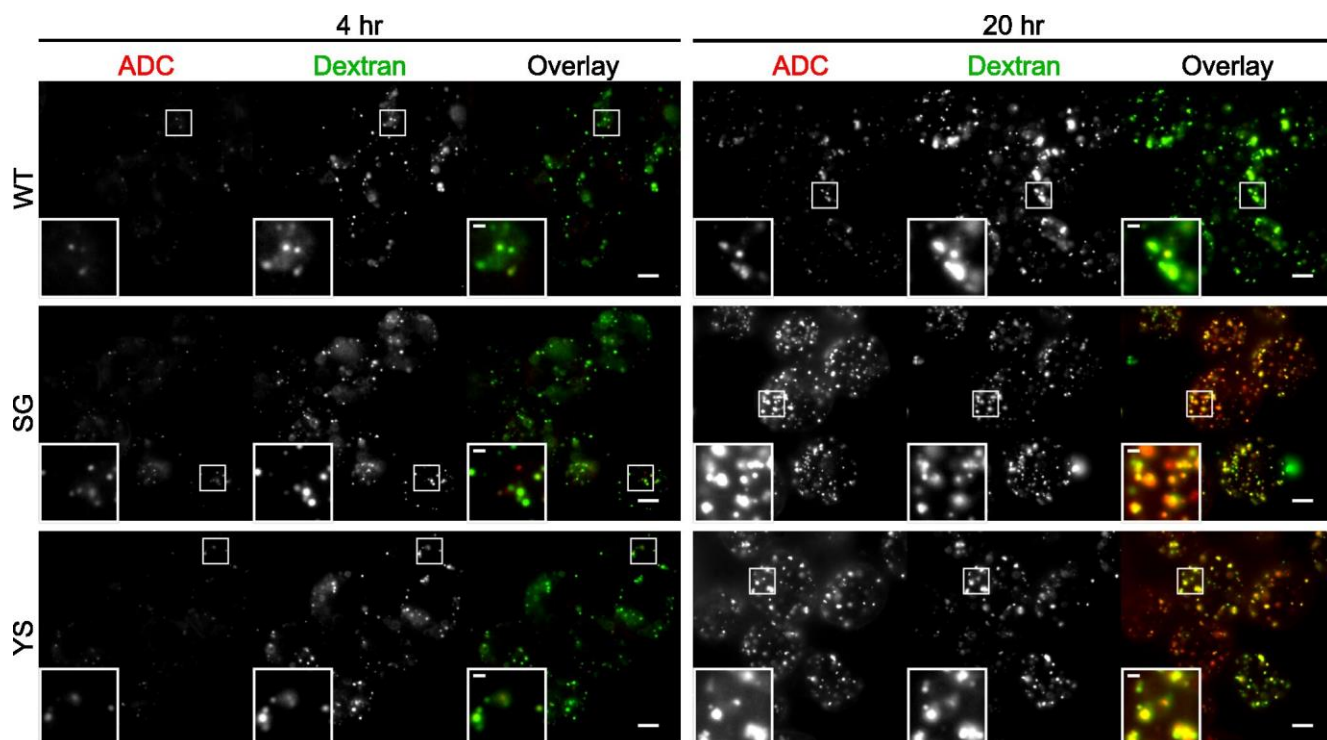


#### Supplementary Figure 7

Cell surface levels of HER2 on cancer cells.

Cells were incubated on ice with 33 nM Alexa 647-labeled pertuzumab (Pertuzumab), an Alexa 647-labeled isotype control (Control IgG), or medium (Untreated) for 30 minutes, washed and analyzed by flow cytometry. Data shown is representative of three independent experiments.

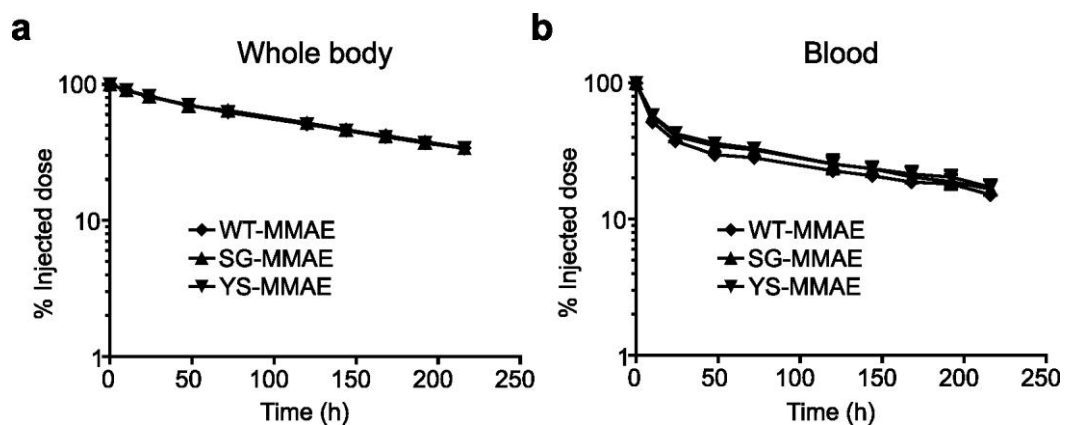




**Supplementary Figure 8**

Acid-switching results in enhanced delivery of ADCs to dextran-positive lysosomes.

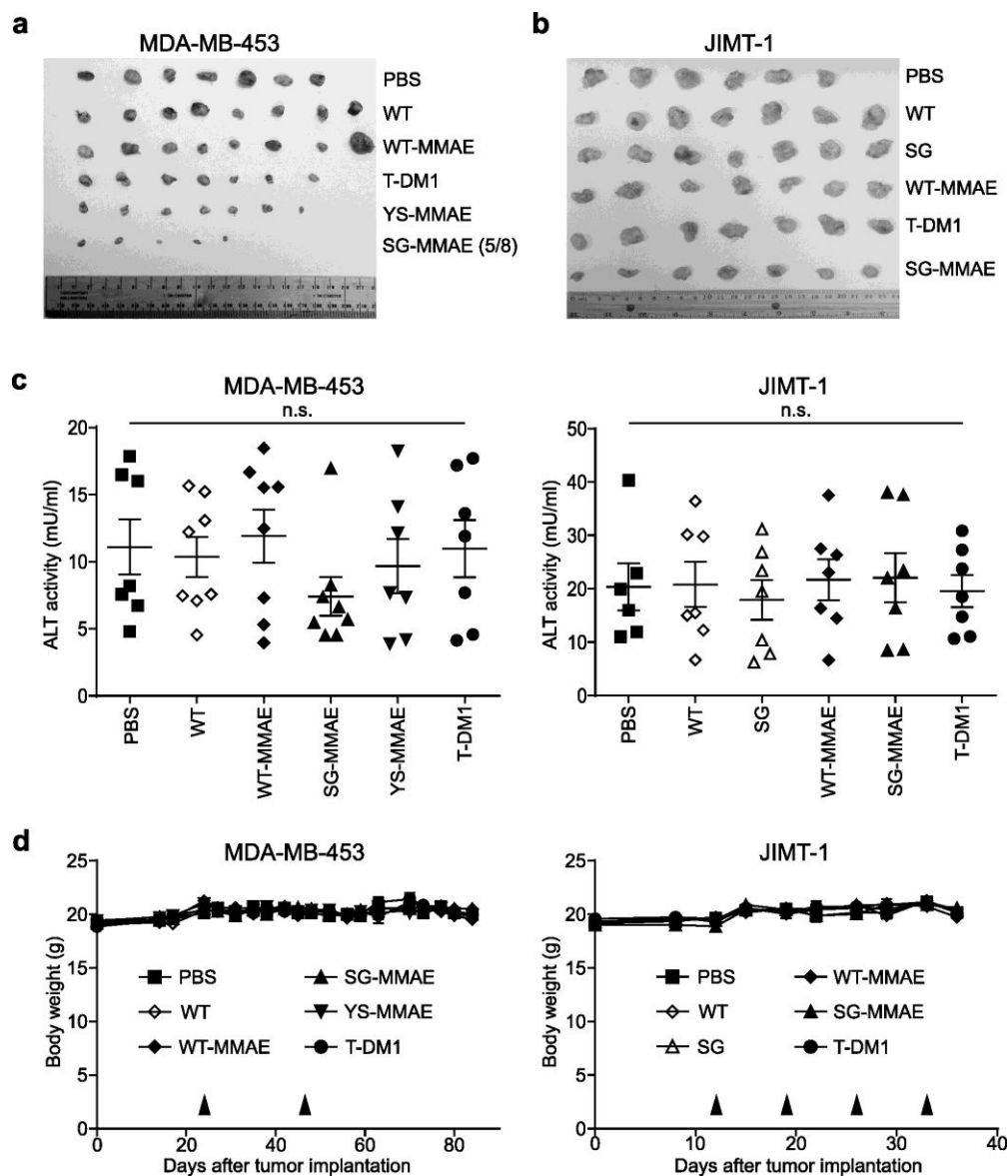
MDA-MB-453 cells were incubated with 5  $\mu$ M Alexa 647-labeled dextran for 2 hours followed by a 3 hour chase period to label lysosomes. Following dextran treatment, cells were incubated with 10 nM Alexa-488 ADCs (WT, SG, and YS) for 4 hours or 20 hours as indicated. Following washing, cells were treated with Alexa 488-specific antibody for 30 minutes on ice to quench cell surface-associated signal. Samples were then fixed and imaged. Cropped regions are expanded in the lower left region of each image. Alexa 488 and Alexa 647 are pseudocolored red and green, respectively, in the overlays. Size bars = 5  $\mu$ m (larger images) or 1  $\mu$ m (insets). Data is representative of two independent experiments and images shown are representative cells ( $n \geq 27$ ).



**Supplementary Figure 9**

Pharmacokinetic behavior of WT-MMAE, SG-MMAE and YS-MMAE.

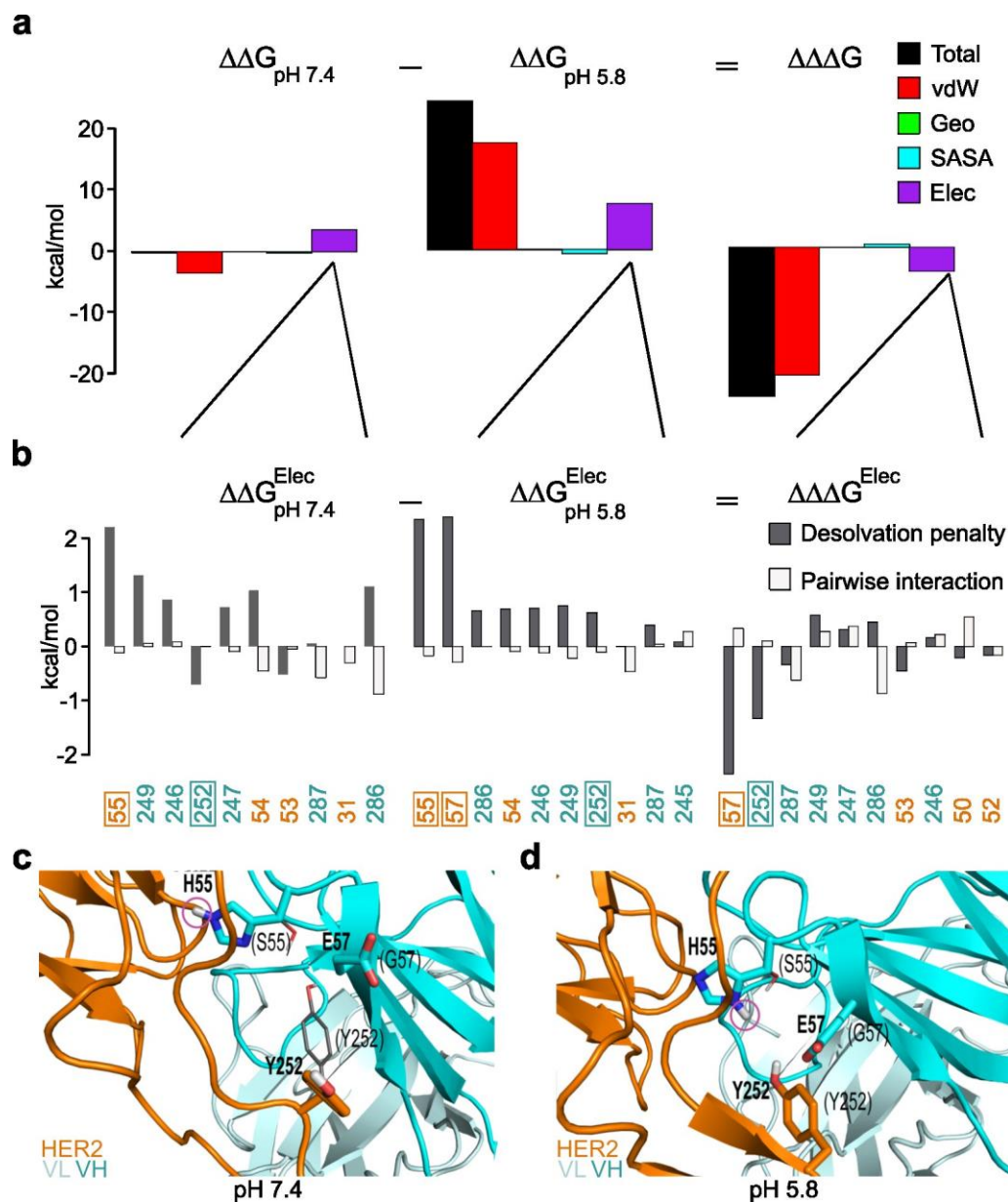
Female BALB/c SCID mice ( $n = 5$  mice/group) were injected intravenously with  $^{125}\text{I}$ -labeled ADC and radioactivity levels in the whole body (**a**) or blood (**b**) were determined at the indicated times. The  $\beta$ -phase half-lives of WT-MMAE, SG-MMAE and YS-MMAE are  $190.6 \pm 4.4$  hours,  $184.4 \pm 11.7$  hours, and  $195.2 \pm 29.5$  hours, respectively (mean  $\pm$  SD; derived from whole body counts). Data shown represent means of normalized counts  $\pm$  SE for mice within each group.



**Supplementary Figure 10**

Analyses of excised tumors, serum alanine aminotransferase (ALT) activity, and body weight of female BALB/c SCID mice following treatment with ADCs.

(a) Female BALB/c SCID mice bearing MDA-MB-453 tumors were treated twice, with a 21 day interval, with 2 mg/kg ADC (WT-MMAE, SG-MMAE or YS-MMAE), T-DM1, unconjugated WT pertuzumab (WT) or PBS ( $n = 7$  mice/group for YS-MMAE, T-DM1 or PBS; 8 mice/group for WT-MMAE, SG-MMAE or WT). (b) JIMT-1 xenografts were treated weekly (four times) with 2 mg/kg ADC (WT-MMAE or SG-MMAE), T-DM1, WT, SG or PBS ( $n = 6$  mice/group for PBS; 7 mice/group for WT-MMAE, SG-MMAE, T-DM1, WT or SG). Tumors from (a) and (b) were extracted and photographed at the end of the experiment. Note that for panel (a), tumors could not be detected in 3 of 8 mice treated with SG-MMAE, and 5 tumors are therefore shown for this treatment group. (c) BALB/c SCID mice were treated as in panels (a) and (b). Blood was collected from mice 4-5 days after the second (MDA-MB-453 xenograft model) or fourth (JIMT-1 xenograft model) dose of ADCs or control and tested for ALT activity, where the units of mU are defined as nmol/min. The mean ALT activity  $\pm$  SE for each group is shown, with the numbers of mice for each treatment group as in panels (a) and (b). No statistical significance (n.s.) was found (one-way ANOVA with Tukey's multiple comparison test;  $P > 0.49$ ). (d) Body weights of BALB/c SCID mice treated as in panels (a) and (b) were determined at the indicated times. Arrowheads indicate treatment days, and mean weight  $\pm$  SE for each group is shown, with the numbers of mice for each treatment group as in panels (a) and (b). Two independent experiments were carried out for panels (a)-(d) with similar results.



**Supplementary Figure 11**

Structural modeling comparing the interaction with HER2 of WT pertuzumab with the acid-switched mutant SG at pH 7.4 and 5.8.

(a) Analyses of the contribution of van der Waals (vdW), geometry (Geo), nonpolar hydration free energy (based on the solvent-accessible surface area, or SASA), and continuum electrostatics (Elec) to the differences in binding free energies ( $\Delta\Delta G$ ) between the SG mutant and WT pertuzumab interacting with HER2 at pH 7.4 and 5.8. (b) Energy decompositions of the Elec interactions shown in (a) for the residues that make the largest energetic contributions to the different binding behavior of WT and SG (HER2 and pertuzumab CDRH2 residues are shown in orange and cyan, respectively), with the most important contributors indicated by boxes. (c,d) The differences in the protonation states (residues His55 and Ser55 of SG and WT, respectively) and conformational states (residue Tyr252 of HER2) between WT pertuzumab and the SG mutant at pH 7.4 (c) and 5.8 (d). The modeled structures of the pertuzumab:HER2 extracellular domain complex are shown, with the pertuzumab VH domain, VL domain and HER2 domain II shown in cyan, light cyan, and orange, respectively. Residues for the SG:HER2 and WT:HER2 complexes are labeled in bold and parentheses, respectively.